



Contents lists available at ScienceDirect

# Quaternary International

journal homepage: [www.elsevier.com/locate/quaint](http://www.elsevier.com/locate/quaint)

## Sakurajima-Satsuma (Sz-S) and Noike-Yumugi (N-Ym) tephras: New tephrochronological marker beds for the last deglaciation, southern Kyushu, Japan

Hiroshi Moriwaki <sup>a,\*</sup>, Takehiko Suzuki <sup>b</sup>, Masanori Murata <sup>b</sup>, Minoru Ikehara <sup>c</sup>, Hiroshi Machida <sup>d</sup>, David J. Lowe <sup>e</sup>

<sup>a</sup> Faculty of Law, Economics and Humanities, Kagoshima University, 1-21-30 Korimoto, Kagoshima 890-0065, Japan

<sup>b</sup> Department of Geography, Tokyo Metropolitan University, Tokyo, Japan

<sup>c</sup> Center for Advanced Marine Core Research, Kochi University, Kochi, Japan

<sup>d</sup> Professor Emeritus, Tokyo Metropolitan University, Tokyo, Japan

<sup>e</sup> Department of Earth and Ocean Sciences, University of Waikato, Private Bag 3105, Hamilton 3240, New Zealand

### ARTICLE INFO

#### Article history:

Available online 9 April 2011

### ABSTRACT

Two prominent tephras, Sakurajima-Satsuma (Sz-S) erupted from Sakurajima volcano and Noike-Yumugi (N-Ym) erupted from Kuchierabujima Island, provide new key marker beds for dating and synchronizing palaeoenvironmental and archaeological records in the last deglaciation in southern Japan. These tephras were identified on the basis of glass major-element compositions in two distal areas, a marine core (IMAGES MD982195) in the northern part of the East China Sea and on the central part of Tanegashima Island, and we related their stratigraphic positions to the marine oxygen isotope-based chronology. In MD982195, Sz-S, 0.8 cm in thickness at 9.12 m depth and N-Ym, 3 cm in thickness at 9.30 m depth, are both white, vitric, ash-grade tephras. On Tanegashima Island, Sz-S, 10 cm in thickness and N-Ym, 3 cm in thickness, are stratigraphically constrained by well-characterised marker tephras Kikai-Akahoya (7300 cal BP) and Aira-Tn (29,000 cal BP). Sz-S is rhyolitic and homogeneous on the basis of glass major-element compositions assayed by electron microprobe. Pumiceous glass shards predominant in distal Sz-S tephra indicate that it derived from pumice fall units that correspond to pumiceous and phreatomagmatic fine ash units constituting proximal Sz-S tephra. N-Ym is rhyolitic and glass major-element analyses reveal compositional diversity between units, suggesting that the lower and middle tephra units dispersed to the east, whereas the upper unit was dispersed north to northwest from the vent.

Stratigraphically, Sz-S occurs at around the start of the late-glacial reversal (cooling) in oxygen isotope records of MD982195, corresponding to the end of GI-1 and the start of GS-1 in the ice-core events of NGRIP (GICC05), consistent with a terrestrial age of ~12,800 cal BP. Based on the oxygen isotope stratigraphy, the tephra identified in the core as N-Ym at 9.30 m depth is close to the end of Greenland GI-1 and hence has an age of ~13,000 cal BP, but on Kuchierabujima Island it has an age based on <sup>14</sup>C assay of charcoal of c. 14,900 cal BP. Although this age discrepancy (14.9 vs 13.0 cal ka) needs resolution, the occurrence in core MD982195 of N-Ym shows that it is more widespread than hitherto demonstrated. The widespread distributions and key stratigraphic positions for the two marker tephras indicate that they are thus critical isochrons for precise correlation of palaeoenvironmental changes and prehistoric cultural events during the last deglaciation in southern Kyushu, and for relating such changes and events to the ice-core chronology via the marine oxygen isotope chronostratigraphy.

© 2011 Elsevier Ltd and INQUA. All rights reserved.

### 1. Introduction

The period from the last glacial to the present interglacial, known as the last deglaciation, is characterised by prominent rapid fluctuations in climate (Björck et al., 1998; Rasmussen et al., 2006, 2008). In order to examine the precise correlation and synchrony or otherwise of such fluctuations in regional to global

\* Corresponding author.

E-mail address: [morih@leh.kagoshima-u.ac.jp](mailto:morih@leh.kagoshima-u.ac.jp) (H. Moriwaki).

contexts, high-resolution ice-core, marine and terrestrial records have been developed through the INTIMATE project both in the North Atlantic region and in Australasia (Turney et al., 2006; Alloway et al., 2007; Hoek et al., 2008). A tephrochronological framework has been developed to help make precise correlations at regional scales during the last deglaciation, and widespread marker tephras, such as Vedde and Borrobol tephras (from Iceland), and the Rerewhakaaitu tephra (from New Zealand), have provided key isochrons for such correlations (Newnham et al., 2003; Lowe, D et al., 2008; Lowe, J et al., 2008).

In Japan, many records for marine and terrestrial palaeoenvironments in the last deglaciation have been obtained (e.g. Arai et al., 1981; Nakagawa et al., 2005; Hayashi et al., 2010). Although numerous tephra beds were deposited during the last deglaciation (Machida and Arai, 2003), relatively few have been identified that enable precise correlations of these marine, terrestrial, and ice-core records to be made. For example, the Ulleung-Oki tephra (10,700 cal BP, Kitagawa et al., 1995; Okuno et al., 2010) from Ulleung Island in Korea, is a useful time marker for correlating Holocene palaeoenvironmental records from the Japan Sea and terrestrial western Japan (Machida and Arai, 1983; Machida et al., 1984a,b). As well, two very widespread marker tephras, Kikai-Akahoya tephra (K-Ah: 7300 cal BP, Kitagawa et al., 1995) and Aira-Tn tephra (AT: 29,000 cal BP, Okuno, 2002) provide key benchmarks throughout Japan and adjacent seas.

In southern Kyushu, one of the most active volcanic regions in Japan, five major volcanic centres including large calderas and associated volcanoes, and the Tokara volcanic islands farther south, align south to north along the Ryukyu Island arc (Fig. 1) (Machida, 2010). More than 20 tephra beds have been recorded from those volcanoes between AT and K-Ah tephras (Moriwaki, 2010). Of these tephras, Sakurajima-Satsuma tephra (Sz-S) from Sakurajima volcano in the Aira volcanic centre (Kobayashi, 1986; Moriwaki, 1992; Machida and Arai, 2003) and Noike-Yumugi (N-Ym) from Kuchierabujima Island on the northern edge of the Tokara volcanic island chain (Geshi and Kobayashi, 2006; Moriwaki et al., 2009), are the most voluminous, suggesting that they may be widespread in occurrence and thus potentially of great use for correlation purposes.

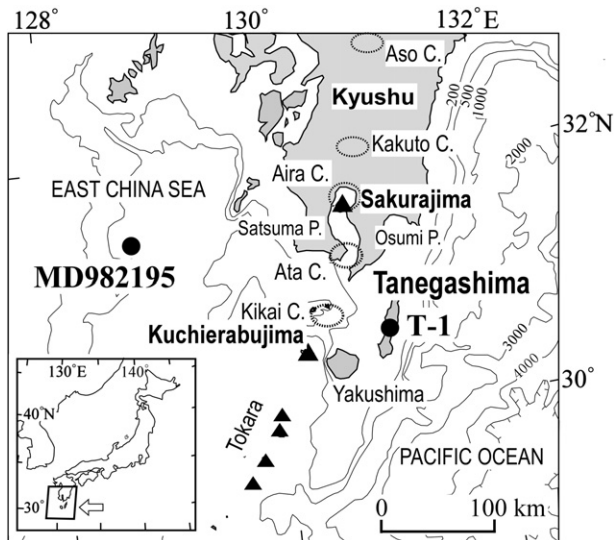


Fig. 1. Study area in the vicinity of southern Japan showing locations of core site MD982195, Kuchierabujima and Tanegashima islands (including site T-1: 30°38'36.35"N, 130°59'24.43"E), and various other volcanoes and calderas (C). Triangles represent volcanoes.

These two tephras were identified in a marine core, IMAGES MD982195 from the northern part of the East China Sea, and on the central part of Tanegashima Island at site T-1. These occurrences are the most distant yet identified of these eruptives (Fig. 1). Here, as part of the programme to develop a chronostratigraphic framework for the Kyushu-INTIMATE project (Integration of ice-core, marine and terrestrial records), the identification of these two tephras was examined on the basis of the chemical composition of glass shards and stratigraphic positions. The relationship of the marine record with the NGRIP ice-core chronology and hence implications for the chronology of the terrestrial palaeoenvironmental and archaeological records in southern Kyushu is discussed.

## 2. Distal occurrences of Sakurajima-Satsuma (Sz-S) and Noike-Yumugi (N-Ym) tephras

### 2.1. MD982195 core

MD982195 is located at 31°38.33'N and 128°56.63'E in the northern part of the East China Sea, 130 km west of Satsuma Peninsula, and in a water depth of 746 m. The core, currently stored at the Center for Advanced Marine Core Research, Kochi University, is 33.65 m in length, and dates back to 40,000 <sup>14</sup>C BP (Ijiri et al., 2005; Fig. 1). Palaeoenvironmental and marine oxygen isotope analyses were carried out on the core (Ijiri et al., 2005; Kawahata et al., 2006). K-Ah and AT tephras were identified at depths of 5.1–6.0 m and 21.8–22.9 m, respectively, and these, together with several <sup>14</sup>C dates, provide the age model for sediments of the last deglacial period (Ijiri et al., 2005). No tephras other than AT and K-Ah have been reported from this core.

MD982195 contains three thin, fine vitric ash beds (denoted A to C) visible within dark silty clay sediments between the AT and K-Ah tephra marker beds (Fig. 2). The uppermost tephra (MD982195-A)

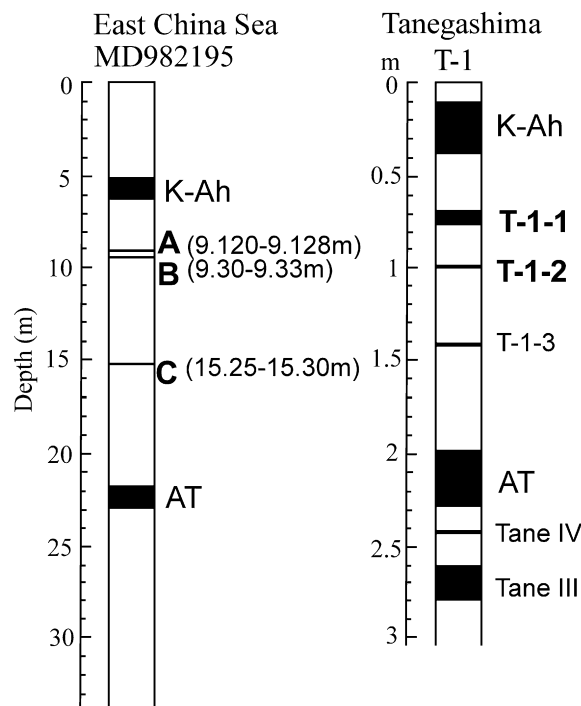


Fig. 2. Late Pleistocene and Holocene tephrostratigraphy in core MD982195 in the East China Sea, including depths of tephras A to C, and on the central part of Tanegashima Island (site T-1), including positions of tephras T-1-1 to T-1-3. K-Ah, Kikai-Akahoya tephra; AT, Aira-Tn tephra. White parts in the sections of the MD982195 and site T-1 denote grey silt and clay sediments, and tephric light-brown soils, respectively.

at 9.120–9.128 m depth comprises an 8-mm thick medium to fine-grained white ash layer that is lenticular in structure. This tephra is dominated by glass shards with minor amounts of primary pyroxene and feldspar. The glass shards contain abundant pumiceous, subordinate fibrous, and minor amounts of bubble-wall glass shards. The maximum grain size of the glass shards is  $\sim 0.3$  mm. According to the age model of this core (Ijiri et al., 2005), the depth 9.120–9.128 m of tephra MD982195-A dates to 13,000 cal BP.

The middle tephra (MD982195-B), finer-grained than the uppermost ash, is pale grey in colour and consists of a patchy ash zone 3 cm thick at 9.30–9.33 m depth. The tephra consists mostly of bubble-wall glass shards. The age model of the core (Ijiri et al., 2005) yields 13,200 cal BP at 9.30–9.33 m, the depth of tephra MD982195-B.

The lowermost tephra (MD982195-C) is dark grey in colour (very similar to the bracketing marine sediments) but is visibly distinguishable as a zone of notably coarse ash at 15.25–15.30 m depth. This tephra contains colorless and brown to pale brown glass shards with a maximum diameter of more than 0.4 mm. The colourless shards consist of pumiceous, fibrous, and platy bubble-walled morphologies in nearly equal proportions, whereas the brown to pale brown shards are dominated by strongly vesicular pumiceous textures and markedly contain non-vesicular chunky textures. The age model of the core (Ijiri et al., 2005) yields 19,800 cal BP at 15.25–15.30 m, the depth of tephra MD982195-C.

## 2.2. Tanegashima Island

Tanegashima Island lies  $\sim 30$  km south of Osumi Peninsula, southern Kyushu Island. At location T-1,  $30^{\circ}38'36.35''$  N,  $130^{\circ}59'24.43''$  E in the central part of the island (Fig. 1), a well-preserved  $\sim 3$ -m-high sequence of late Pleistocene tephra beds includes the K-Ah and AT tephtras. Three tephra beds, T-1-1, T-1-2, and T-1-3 (from upper to lower) occur between them (Fig. 2). The uppermost tephra (T-1-1) is a fine-grained vitric ash bed, 10 cm thick and orange in colour. The middle tephra (T-1-2) is 3 cm thick and coarser-grained than T-1-1. It contains dominantly grey and orange pumice clasts, which reveal compositional diversity (see analyses below). The lowermost tephra (T-1-3), dark grey in colour, is a fine scoriaceous ash bed.

## 2.3. Possible correlatives for the newly-discovered distal tephtras

Tephrostratigraphic frameworks spanning the last deglaciation have been erected for each volcanic centre in southern Kyushu based on proximal stratigraphies (Okuno, 2002; Machida and Arai, 2003; Moriwaki, 2010). Of these proximal tephtras, the most likely correlatives of tephtras MD982195-A and MD982195-B, and of tephtras T-1-1 and T-1-2 – in terms of stratigraphy and volume – are Sakurajima-Satsuma tephtra (Sz-S) erupted from Sakurajima volcano in the Aira volcanic centre (Kobayashi, 1986; Moriwaki, 1992) and Noike-Yumugi tephtra (N-Ym) erupted from Kuchierabujima Island situated at the northern tip of the Tokara volcanic chain (which includes seven major active volcanic islands) (Fig. 1) (Geshi and Kobayashi, 2006; Moriwaki et al., 2009).

Sz-S is the most voluminous of  $\sim 17$  tephtras erupted from Sakurajima volcano in the past  $\sim 26,000$  cal yrs (Kobayashi, 1986; Moriwaki, 1994, 2010). It is estimated to be  $\sim 11$  km<sup>3</sup> in bulk volume (Kobayashi and Tameike, 2002). It consists of more than 10 members, which are mostly pumice fall beds together with a pair of phreatomagmatic fine-grained ash-fall beds and a base surge deposit (Moriwaki, 1992) (Figs. 1 and 3). Sz-S occurs not only in the Osumi Peninsula, on which most tephtras prevail eastward from source vents because of prevailing westerlies, but also notably on the Satsuma Peninsula westward from Sakurajima volcano,

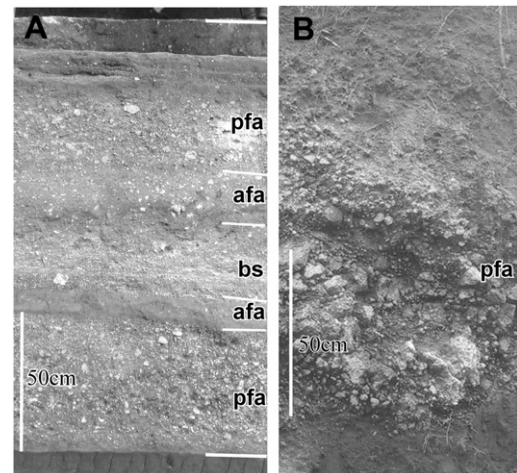


Fig. 3. Defined members of (A) Sakurajima-Satsuma tephtra on Satsuma Peninsula and (B) Noike-Yumugi tephtra on Kuchierabujima Island. pfa: pumice fall; afa: ash fall; bs: base surge deposit.

collectively forming a circular distribution pattern (Kobayashi, 1986; Moriwaki, 1992).

Regarding the age of Sz-S, 10,500 <sup>14</sup>C BP was given on the basis of several dates for charcoal in Sz-S measured by the beta counting (liquid scintillation) method (Machida and Arai, 1992). Okuno et al. (1997) estimated the age of Sz-S as 11,500 <sup>14</sup>C BP on the basis of dates obtained by the AMS dating method on humic soils immediately below Sz-S. Okuno (2002) determined a calibrated age of 12,800 cal BP for Sz-S on the basis of a revised <sup>14</sup>C age of 11,000 <sup>14</sup>C BP. This last age is the only calibrated age obtained thus far for the Sz-S tephtra, hence 12,800 cal BP is used for the terrestrial age of Sz-S in this paper. Although Okuno et al. (1997) considered the gap of 1000 years between 10,500 and 11,500 <sup>14</sup>C BP probably to be due to the different methods of assay (i.e., beta counting vs. AMS), it may alternatively be attributable to differences in sample types and their stratigraphic juxtapositions i.e., assay of humic material in soils below Sz-S vs. charcoal within Sz-S. The dating of Sz-S tephtra deposits needs further examination to improve the precision of their eruptive age.

N-Ym was erupted from the Noike vent in the Kuchierabujima volcanic complex, located in the central part of Kuchierabujima Island (Geshi and Kobayashi, 2006) (Figs. 1 and 3). The tephrostratigraphic position of N-Ym is constrained by K-Ah (above) and AT (below) (Geshi and Kobayashi, 2006; Moriwaki et al., 2009). N-Ym consists of pumice fall deposits underlying a thin pyroclastic flow deposit and contains banded pumices and scoriae showing compositional diversity. These fall and flow units constitute a single tephtra formation without a time gap between the units. The maximum thickness for the entire deposit exceeds 5 m around the vent, and it is the most voluminous of the tephtras erupted from the Tokara volcanic chain during the last deglaciation (Geshi and Kobayashi, 2006; Moriwaki et al., 2009). The N-Ym eruption probably attained a VEI of 6, judging from the widespread occurrences revealed in this paper. The isopachs on Kuchierabujima Island show the main distributions to have been north and east of the vent.

N-Ym is dated between 15,560 and 14,280 cal BP (median  $\sim 14,900$  cal BP) on the basis of a <sup>14</sup>C age ( $12,600 \pm 70$  <sup>14</sup>C BP) obtained on charcoal in the pumice fall deposit (Moriwaki et al., 2009), and between 14,900 and 14,150 cal BP (median  $\sim 14,500$  cal BP) on the basis of a <sup>14</sup>C age ( $12,440 \pm 60$  <sup>14</sup>C BP) on charcoal in the pyroclastic flow deposit on the island (Geshi and Kobayashi, 2006). Kobayashi et al. (2002) obtained an age of

12,435 ± 50 <sup>14</sup>C yr BP on charcoal in the pumice fall deposit. Although those ages show relatively good agreement, their precision is insufficient for examining the high-resolution chronology required for palaeoenvironmental reconstructions. It is necessary both to collect more high-precision dates on optimum dating material for N-Ym and Sz-S, and to employ a Bayesian statistical approach to calibrate sequences of ages using flexible age-sediment modeling. Such modelling provides enhanced and more precise chronologies expressed as probabilities (e.g., Wohlfarth et al., 2006; Blockley et al., 2008; Lowe, D. et al., 2008).

### 3. Characterization and identification

Glass chemical compositions are typically used to identify distal tephtras (Lowe, 2011). Major-element compositions of the glass shards were obtained for the three distal tephtras in core MD982195 and at T-1 on Tanegashima Island using electron microprobes of Kagoshima University, Tokyo Metropolitan University, and the University of Toronto. Conditions of analysis are noted in Table 1. Any small differences in composition relating to the deployment of these different instruments were checked using glass shards of AT tephtra (Table 1), which is very homogeneous with respect to major elements and thus provides a useful in-house standard for checking analytical reproducibility (Machida and Arai, 2003). Analyses of AT glass shards showed that the electron microprobe of Tokyo Metropolitan University underestimated both CaO (by 0.43 wt%, mean value) and Na<sub>2</sub>O (by 0.56 wt%), and overestimated K<sub>2</sub>O (by 0.28 wt%) in comparison with analyses obtained using the electron microprobes at the University of Toronto and Kagoshima University. Other oxides, however, are essentially concordant between the three instruments (Table 1). Therefore, correction factors were applied for these three oxides for the glass major-element compositions of tephtras MD982195-A, -B and -C that were analysed at Tokyo Metropolitan University (Figs. 4 and 5). The major-element compositions of glass obtained from samples of the Sz-S and N-Ym tephtras at proximal reference localities are given in Table 2. Analyses of glass shards from samples of the distal tephtras MD982195-A, -B and -C (analysed at Tokyo Metropolitan

University), and from T-1-1 and T-1-2 on Tanegashima Island (analysed at Kagoshima University), are shown in Table 3. All data are normalized to a 100%-water-free basis.

#### 3.1. Sakurajima-Satsuma (Sz-S) tephtra

The average major-element compositions (Table 2) and oxide bivariate plots using the major elements of individual glass shards (Fig. 4) show that the major-element compositions analysed for several members of Sz-S at reference sites on the Osumi and Satsuma peninsulas are very similar, demonstrating they are derived from homogeneous magma: the major elements of glass from all members of Satsuma and Osumi peninsulas lie within 74–76 wt% for SiO<sub>2</sub>, 13–14 wt% for Al<sub>2</sub>O<sub>3</sub>, 0.2–0.6 wt% for TiO<sub>2</sub>, 1.6–2.2 wt% for FeO<sub>t</sub>, 1.5–2.5 wt% for CaO, and 2.7–3.2 wt% for K<sub>2</sub>O. Thus it is not possible to distinguish between the members on Osumi and Satsuma peninsulas on the basis of the major-element compositions. The Sz-S glasses are classified as high-silica-rhyolite (LeBas et al., 1986).

Figure 4 and Table 3 show that the uppermost tephtra bed, MD982195-A in the northern part of the East China Sea, and tephtra T-1-1 on Tanegashima Island, are similar in composition to the proximal Sz-S tephtras, indicating that these two distal tephtra beds are likely correlatives of Sz-S tephtra. Although it is impossible to correlate the distal tephtras to specific members of Sz-S using glass-shard major elements alone (because glasses of the Sz-S members are effectively all identical compositionally with regard to major elements), the predominance of pumiceous glass shards in the distal tephtra bed MD982195-A suggests that it is derived from plinian fall-out pumice members (Fig. 3).

#### 3.2. Noike-Yumugi (N-Ym) tephtra

Proximal N-Ym is classed as a rhyolite (Table 2) (LeBas et al., 1986). However, the major-element compositions of N-Ym are diverse, not only stratigraphically but also within the same member as evidenced by the wide values for standard deviation (Moriwaki et al., 2009: Table 2, Fig. 5). The values in the six diagrams (Fig. 5) show a wide dispersion and distinctively bimodal composition (Moriwaki et al., 2009). Upper, middle, and lower units are classed (using non-normalised compositions) as a rhyolite, a dacite and a rhyodacite, respectively (LeBas et al., 1986). For example, the upper unit (KU5) of N-Ym shows bimodal composition in the SiO<sub>2</sub>–Al<sub>2</sub>O<sub>3</sub> diagram: one mode with high SiO<sub>2</sub> (77–79 wt%) and low Al<sub>2</sub>O<sub>3</sub> (11.9–12.5 wt %), and the other, low SiO<sub>2</sub> (74 wt%) and high Al<sub>2</sub>O<sub>3</sub> (13 wt%), and one with high TiO<sub>2</sub> (0.5–0.7 wt%) and high FeO<sub>t</sub> (2.4–2.5 wt%), and the other, low TiO<sub>2</sub> (0.14–0.4 wt%) in the FeO<sub>t</sub>–TiO<sub>2</sub> diagram. Similarly, the middle unit (KU4) has a wide range in composition with low SiO<sub>2</sub> (72–75 wt %) and high Al<sub>2</sub>O<sub>3</sub> (12.8–14.2 wt%) in the SiO<sub>2</sub>–Al<sub>2</sub>O<sub>3</sub> diagram, and high TiO<sub>2</sub> (0.5–0.8 wt%) and high FeO<sub>t</sub> (2.7–3.8 wt%) in the FeO<sub>t</sub>–TiO<sub>2</sub> diagram. The lower unit (KU2) shows a narrow range in composition with low SiO<sub>2</sub> (74–76 wt%) and high Al<sub>2</sub>O<sub>3</sub> (12.7–13.1 wt%) in the SiO<sub>2</sub>–Al<sub>2</sub>O<sub>3</sub> diagram, and wide range for TiO<sub>2</sub> but narrow for FeO<sub>t</sub> in composition with relatively high TiO<sub>2</sub> (0.3–0.7 wt %) and relatively high FeO<sub>t</sub> (2.3–2.7 wt%) (Fig. 5). Such heterogeneity is consistent with the occurrences of banded pumices and scoriae in N-Ym tephtra bed at the proximal reference locations described earlier.

The distal tephtras, T-1-2 on Tanegashima and tephtras MD982195-B and MD982195-C in the East China Sea, are classified as high-silica rhyolites based on glass major-element compositions (Table 3) (LeBas et al., 1986). Significantly lower CaO and higher K<sub>2</sub>O contents for tephtras MD982195-B and MD982195-C, relative to those of tephtra T-1-2, are possibly due to the differences resulting from the different electron microprobes used, as evidenced by the

**Table 1**  
Average major-element composition of glass shards from Aira-Tn (AT) tephtra, used as an in-house standard for electron microprobe analysis.

Tephtra name	AT	AT	AT
Sample number	KU1 & KU35	UT1304 & UT1305	AT091224
Laboratory	Kagoshima Univ.	Univ. of Toronto	Tokyo Metropolitan Univ.
SiO <sub>2</sub>	77.95 (0.25)	78.13 (0.22)	78.91 (0.39)
Al <sub>2</sub> O <sub>3</sub>	12.45 (0.15)	12.21 (0.14)	12.09 (0.11)
TiO <sub>2</sub>	0.14 (0.07)	0.13 (0.03)	0.14 (0.05)
FeO <sub>t</sub>	1.24 (0.05)	1.26 (0.05)	1.28 (0.11)
MnO	0.03 (0.02)	0.05 (0.03)	0.08 (0.04)
MgO	0.11 (0.05)	0.12 (0.01)	0.11 (0.04)
CaO	1.15 (0.05)	1.16 (0.05)	0.72 (0.06)
Na <sub>2</sub> O	3.51 (0.17)	3.62 (0.11)	3.03 (0.35)
K <sub>2</sub> O	3.43 (0.18)	3.33 (0.07)	3.66 (0.10)
H <sub>2</sub> O <sub>d</sub>	3.43 (0.79)	5.34 (0.29)	6.34 (1.52)
n	15	30	12

Notes: Analyses undertaken on a Cameca SX-50 wavelength dispersive microprobe at University of Toronto, on a JXA-8600SX at Kagoshima University, and on a JEOL JED-2300 energy dispersive X-ray spectrometer at Tokyo Metropolitan University. Operating conditions are 15 kV accelerating voltage, 10 μm beam diameter and 10 nA beam current for University of Toronto and Kagoshima University, and 15 kV accelerating voltage, 10 μm beam diameter and 1.2 nA beam current for Tokyo Metropolitan University. Standardization achieved using mineral and glass standards. Analyses normalized to 100% on a water-free basis. H<sub>2</sub>O<sub>d</sub> = water by difference; total iron expressed as FeO<sub>t</sub>; (#) = standard deviation; n = number of shards analysed.

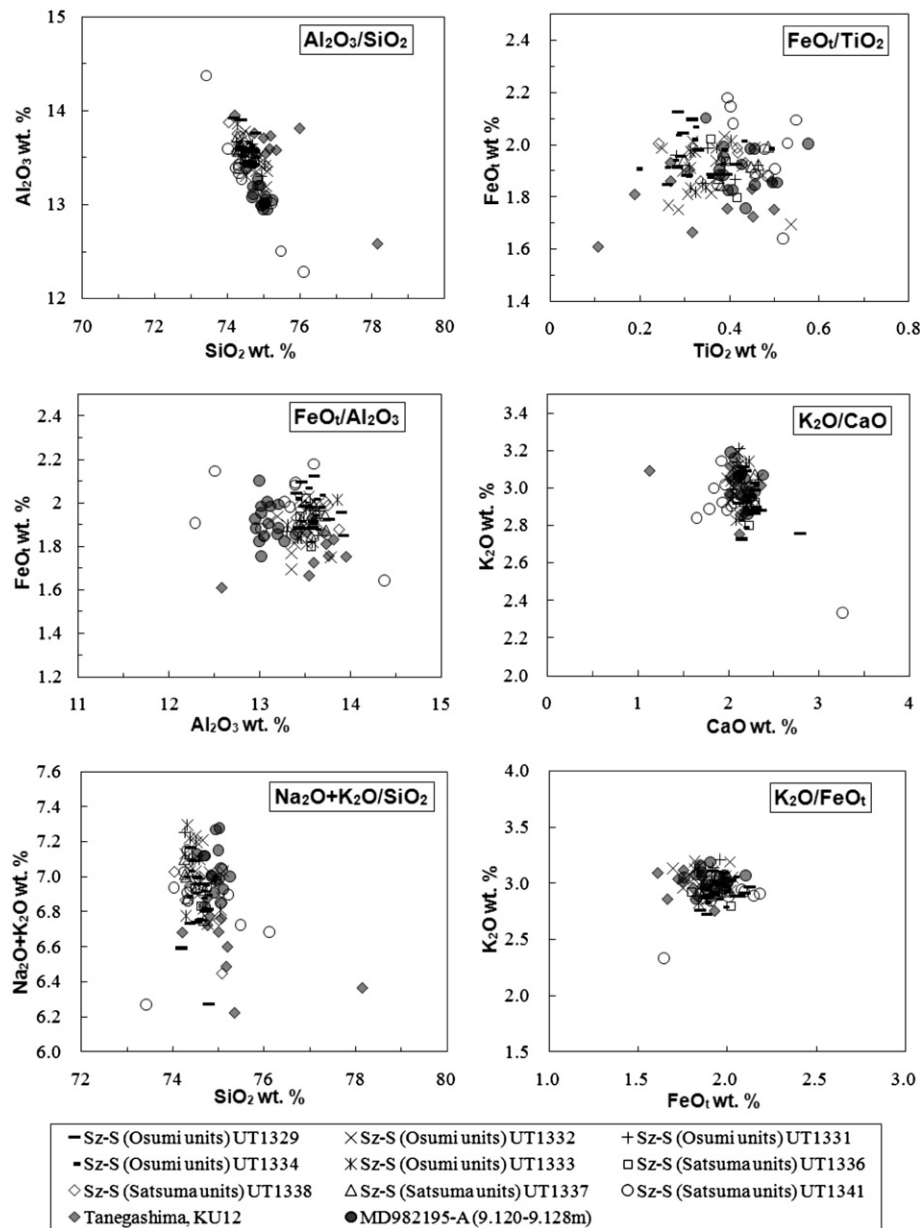


**Fig. 4.** Oxide variation diagrams of glass composition (wt%) showing correlation of Sakurajima-Satsuma (Sz-S) tephra (including samples from sites on Osumi and Satsuma peninsulas) with unknown late Pleistocene tephtras on Tanegashima Island and at MD982195 in the East China Sea. The electron microprobe analyses for tephra MD982195-A, analysed at TMU, were corrected using analyses of glass from Aira-Tn tephra (see text).

AT glass chemical compositions (analyses in Table 3 are reported uncorrected). The wide compositional range present in samples from tephtras T-1-2, MD982195-B, and MD982195-C, combined with the limited number of analyses obtainable, make it difficult to directly compare the resulting average composition with the proximal composition of N-Ym tephra bed. This wide compositional range is reflected in the large standard deviations obtained for these samples. The proximal pumice fall deposits of N-Ym are similarly diverse. In these circumstances, the distribution of individual glass shards analyses can be used to characterize tephtras MD982195-B, MD982195-C, and T-1-2, and to explore potential correlations amongst themselves and the N-Ym tephra bed (Fig. 5).

The values in the six biplots (Fig. 5) show a wide dispersion and distinctively bimodal composition in every ash bed, which mimic those of the proximal N-Ym pumice fall deposits on Kuchierabujima Island (Moriwaki et al., 2009) and collectively reveal similar patterns

in both distal and proximal tephtras. In more detail, tephra T-1-2 on Tanegashima Island is compositionally similar to the middle and lower units of the proximal N-Ym tephra bed on Kuchierabujima Island, as exemplified in the  $\text{SiO}_2\text{--Al}_2\text{O}_3$  diagram with contents of low  $\text{SiO}_2$  (75–76 wt%) and high  $\text{Al}_2\text{O}_3$  (12.7–13.4 wt%), and, in the  $\text{FeO}_t\text{--TiO}_2$  diagram, high  $\text{TiO}_2$  (0.29–0.59 wt%) and high  $\text{FeO}_t$  (2.3–2.5 wt%). Tephra T-1-2 is likely correlated to these units, thus showing that lower and middle units of N-Ym fall-out pumice were dispersed eastward from the vent.

Tephtras MD982195-B and MD982195-C, although stratigraphically separated by ~ 6 m (Fig. 2), are both similar compositionally to the upper unit of N-Ym. In particular, glass analyses (of B and C) match one of the bimodal populations of N-Ym as exemplified in the  $\text{SiO}_2\text{--Al}_2\text{O}_3$  and  $\text{FeO}_t\text{--TiO}_2$  diagrams (Fig. 5), which shows prominently high  $\text{SiO}_2$  (77–79 wt%) and low  $\text{Al}_2\text{O}_3$  (11.7–12.3 wt%) in the first population, and low  $\text{SiO}_2$  (72–76 wt%) and high  $\text{Al}_2\text{O}_3$

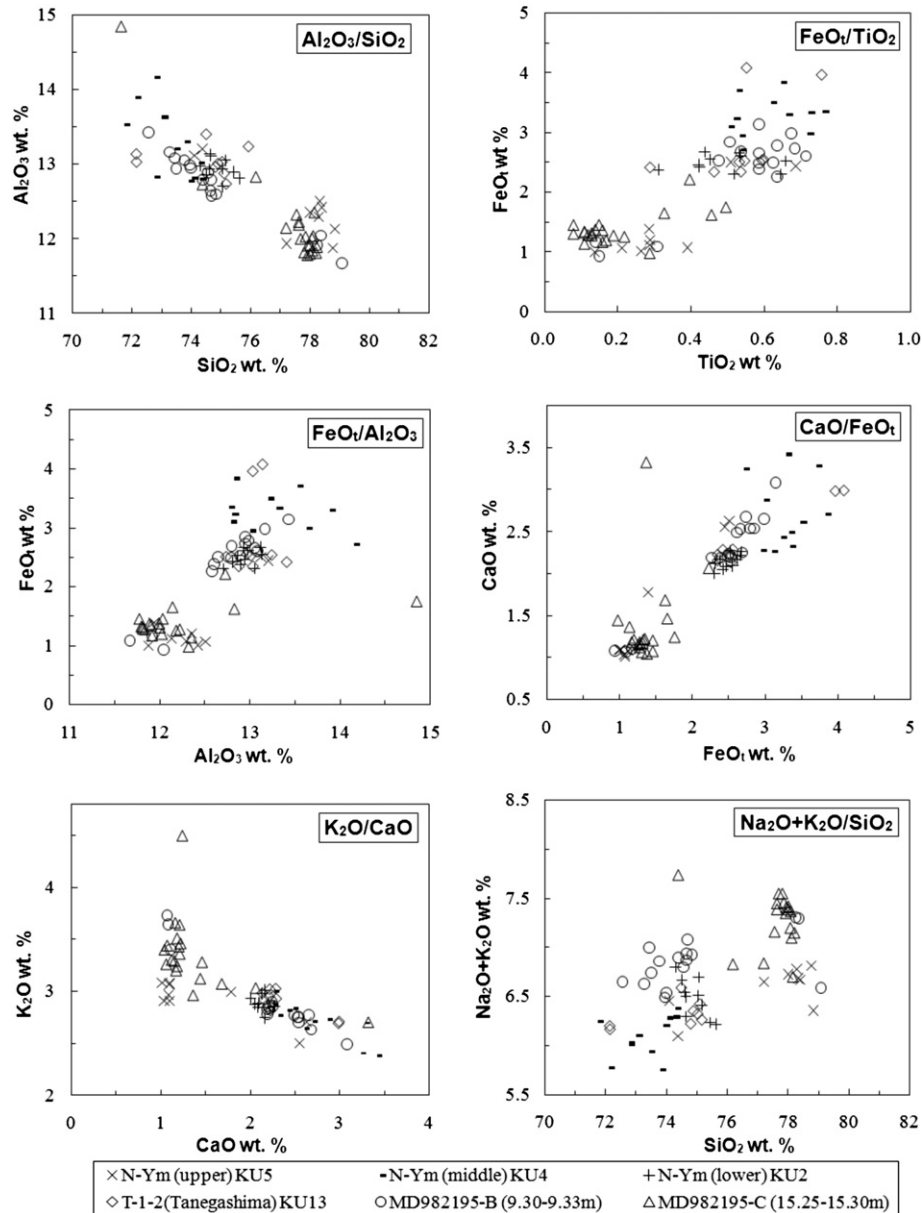


**Fig. 5.** Oxide variation diagrams of glass composition (wt%) showing correlation of Noike-Yumugi (N-Ym) tephra (upper, middle, and lower units) with unknown late Pleistocene tephras on Tanegashima Island and at MD982195 in the East China Sea. The electron microprobe analyses for tephra MD982195-B and -C, analysed at TMU, were corrected using analyses of glass from Aira-Tn tephra (see text).

**Table 2**  
Average major-element composition (normalized) of glass shards from proximal N-Ym tephra on Kuchierabujima Island and from proximal Sz-S tephra on Osami and Satsuma peninsulas, southern Kyushu.

Tephra name (Location) Stratigraphy (Reference No.)	N-Ym (Kuchierabujima <sup>a</sup> )			Sz-S (Osami Peninsula)	Sz-S (Satsuma Peninsula)
	Upper (KU5)	Middle (KU4)	Lower (KU2)		
$SiO_2$	77.37 (1.84)	73.29 (0.87)	74.90 (0.42)	74.58 (0.23)	74.58 (0.48)
$Al_2O_3$	12.43 (0.47)	13.27 (0.48)	12.94 (0.17)	13.53 (0.16)	13.48 (0.35)
$TiO_2$	0.34 (0.17)	0.61 (0.09)	0.49 (0.09)	0.34 (0.07)	0.39 (0.09)
$FeO_t$	1.42 (0.61)	3.27 (0.33)	2.47 (0.18)	1.93 (0.09)	1.94 (0.11)
MnO	0.06 (0.06)	0.10 (0.04)	0.06 (0.05)	0.07 (0.03)	0.05 (0.03)
MgO	0.31 (0.24)	0.64 (0.16)	0.48 (0.05)	0.42 (0.03)	0.52 (0.16)
CaO	1.49 (0.67)	2.72 (0.43)	2.14 (0.11)	2.18 (0.12)	2.15 (0.24)
$Na_2O$	3.67 (0.12)	3.38 (0.18)	3.61 (0.17)	3.96 (0.15)	3.96 (0.12)
$K_2O$	2.91 (0.19)	2.71 (0.19)	2.88 (0.06)	2.99 (0.11)	2.93 (0.13)
$H_2O_d$	4.50 (1.90)	8.26 (3.67)	5.72 (1.38)	4.55 (1.22)	6.56 (1.83)
n	9	11	10	47	29

<sup>a</sup> After Moriwaki et al. (2009). Analysed at Kagoshima University for N-Ym and at the University of Toronto for Sz-S. See Table 1 for conditions of analysis.

**Table 3**

Average major-element composition (normalized) of glass shards from tephra A (correlated here with Sakurajima-Satsuma tephra, Sz-S), tephra B (correlated here with Noike-Yumugi tephra, N-Ym), and tephra C (uncorrelated) in core MD982195, and of glass shards from samples T-1-1 (correlated here with Sz-S) and T-1-2 (correlated here with N-Ym) at site T-1 on Tanegashima Island.

Location	MD982195			Tanegashima	
	A	B	C	T-1-1	T-1-2
Sample name					
Sample depth	9.120–9.128 m	9.30–9.33 m	15.25–15.30 m	68 cm	98 cm
Reference No.	No.142-1	No.142-2	No.142-3	KU12	KU13
SiO <sub>2</sub>	75.51 (0.18)	75.47 (1.95)	77.92 (1.61)	75.31 (1.04)	74.41 (1.35)
Al <sub>2</sub> O <sub>3</sub>	13.20 (0.13)	12.82 (0.48)	12.32 (0.69)	13.58 (0.36)	13.05 (0.20)
TiO <sub>2</sub>	0.43 (0.06)	0.53 (0.18)	0.20 (0.13)	0.34 (0.13)	0.54 (0.12)
FeO <sub>t</sub>	1.93 (0.09)	2.38 (0.69)	1.40 (0.27)	1.79 (0.10)	2.81 (0.69)
MnO	0.08 (0.04)	0.09 (0.06)	0.08 (0.05)	0.07 (0.04)	0.07 (0.04)
MgO	0.38 (0.06)	0.40 (0.18)	0.15 (0.10)	0.40 (0.12)	0.57 (0.17)
CaO	1.74 (0.09)	1.76 (0.60)	0.95 (0.52)	2.02 (0.32)	2.39 (0.34)
Na <sub>2</sub> O	3.42 (0.15)	3.35 (0.33)	3.36 (0.54)	3.52 (0.44)	3.27 (0.49)
K <sub>2</sub> O	3.32 (0.08)	3.20 (0.35)	3.62 (0.38)	2.97 (0.11)	2.89 (0.13)
H <sub>2</sub> O <sub>d</sub>	4.16 (1.03)	5.31 (2.41)	5.24 (2.15)	3.62 (1.28)	1.59 (0.84)
n	16	16	20	10	10

Tephra MD982195-A, -B, -C were analysed at Tokyo Metropolitan University. Values for oxides of Ca, Na, and K are those obtained before corrections using AT glass compositions as an in-house standard (see text). Tephra from Tanegashima were analysed at Kagoshima University. See Table 1 for conditions of analysis.

(13.4–12.6 wt%) in the second population (although the values in the second population are rather dispersed), and low FeO<sub>t</sub> (0.9–1.8 wt%) and low TiO<sub>2</sub> (0.1–0.5 wt%) in the first population and high FeO<sub>t</sub> (2.2–3.1 wt%) and high TiO<sub>2</sub> (0.4–0.7 wt%) in the second population. Considering the stratigraphic juxtapositions of the two tephra beds, tephra MD982195-B is likely correlated with the upper unit of the N-Ym tephra as at proximal locations, although it is difficult to show that it is distinctly different from tephra MD982195-C by the use of major-element compositions alone.

Tephra MD982195-C, aged ~19,800 cal BP on the basis of the marine oxygen isotope stratigraphy (Fig. 6), is a different tephra bed derived probably from an eruption on Kuchierabujima Island. The correlation of tephra MD982195-B with the upper units of N-Ym fall-out tephra indicates that these eruptives were dispersed north to northwestward from Kuchierabujima Island.

Thus, tephra deposits such as tephra MD982195-B, which is heterogeneous in composition, nevertheless have the potential to be correlated although the analytical data require careful examination (Shane et al., 2003, 2008; Lowe, D. et al., 2008).

## 4. Implications

### 4.1. Stratigraphic positions with respect to marine oxygen isotope record and age relationships

The Sz-S and N-Ym tephra, correlated here with tephra MD982195-A and MD982195-B, respectively, can be related stratigraphically to changes evident in the marine oxygen isotope record for the last deglaciation in the same core (Fig. 6; Ijiri et al., 2005).

Tephra Sz-S occurs at around the start of the late-glacial reversal (cooling) in the oxygen isotope records of MD982195 (Ijiri et al., 2005) and an approximate peak in abundance of arboreal pollen (Kawahata and Oshima, 2004), which in turn corresponds to the end of GI-1 and the start of GS-1 in the ice-core events of NGRIP (GICC05) (Lowe, J. et al., 2008). The age model of MD982195 core (Ijiri et al., 2005) generates an age for tephra Sz-S as ~13,000 cal BP, as noted earlier. Given that the transition peaks of the isotopic records of MD982195 and NGRIP (GICC05) are simultaneous, the age of Sz-S is estimated at ~13,000–12,800 cal BP according to the age of the peak in NGRIP/GICC05, which nearly corresponds to that of the age model of MD982195.

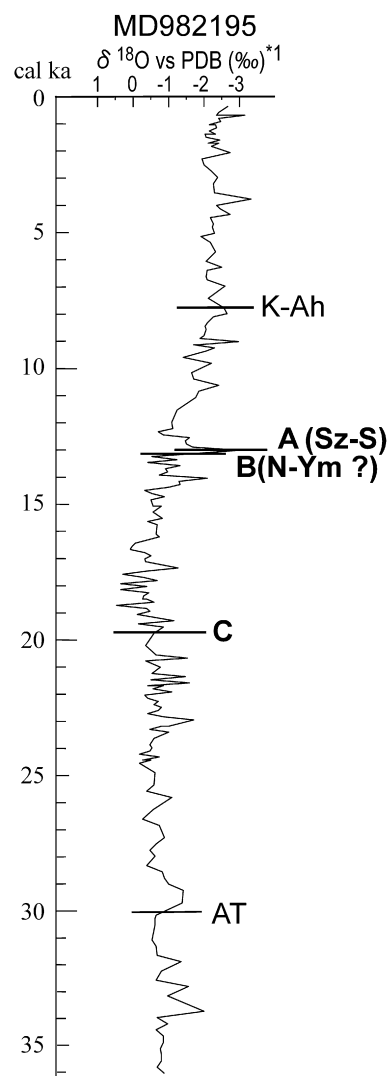


**Fig. 6.** Stratigraphic positions of (A) Sakurajima-Satsuma (Sz-S) and (B) Noike-Yumugi (N-Ym) tephra with respect to the marine oxygen isotope records in core MD982195. Also shown is position of tephra C (uncorrelated), aged c. 20,000 cal BP. \*1, Marine oxygen isotope curve and stratigraphic positions of AT and K-Ah are after Ijiri et al. (2005). Note that the ages of AT and K-Ah slightly differ from those described in the text, which are probably more suitable.

The age of tephra Sz-S, estimated on land at 12,800 cal BP (Okuno, 2002), nearly coincides with that based on  $^{14}\text{C}$  ages recorded in the marine core (Ijiri et al., 2005), and matches in age the approximate boundary between the events GI-1a and GS-1 in the NGRIP/GICC05 isotopic records (Lowe, J. et al., 2008; Rasmussen et al., 2008). Thus, the equivalent stratigraphic position of tephra Sz-S in the NGRIP ice-core records nearly corresponds to both the  $^{14}\text{C}$  age of Sz-S obtained from terrestrial records and that derived from the marine oxygen isotope record of MD982195. At a higher resolution scale, there are slight differences in age between the records, mainly relating to the position of the boundary of events GS-1 and GI-1, or GI-1a. Although such a difference may in theory be due to a climatic change being recorded in the East China Sea before such a change was recorded in Greenland, it is more likely a result of the relative imprecision of the  $^{14}\text{C}$  ages thus far obtained on Sz-S. Obtaining a more precise age for Sz-S will allow the age models for the marine record to be improved.

In contrast, based on oxygen isotope stratigraphy, tephra MD982195-B identified in the core as N-Ym at 9.30–9.33 m depth occurs near the end of Greenland GI-1, which has an age of  $\sim 13,200$  cal BP using the age model of the marine core (Ijiri et al., 2005; Lowe, J. et al., 2008) (Fig. 6). Given that the transition peaks of the isotopic records of MD982195 and NGRIP (GICC05) are simultaneous, the age of N-Ym is estimated at 13,000–13,200 cal BP, which nearly corresponds to that of the age model of MD982195 (Ijiri et al., 2005). However, the age of N-Ym on land is estimated at 14,900–14,500 cal BP. Although this age discrepancy (14.9–14.5 vs. 13.0–13.2 cal ka) needs resolution, the occurrence in core MD982195 of N-Ym, assuming the correlation is sound, shows that it is more widespread than hitherto demonstrated.

These newly identified occurrences of Sz-S and N-Ym tephtras in the marine core provide potential for examining the relationship between regional palaeoenvironments including climatic changes of southern Kyushu and how such changes relate to the ice-core chronostratigraphy. Thus tephtras Sz-S and N-Ym supplement previously well-known marker tephtras K-Ah and AT and together provide an enhanced tephrochronological framework to enable marine, ice and terrestrial records to be linked, as occurs for records of the last deglaciation in the North Atlantic and elsewhere (Lowe and Hoek, 2001; Lowe, J. et al., 2008; Lowe, D. et al., 2008).

#### 4.2. Distributions of Sz-S and N-Ym tephtras

Core MD982195 and the central part of Tanegashima Island lie c. 190 km west and c. 120 km south of the Sz-S source vent, Sakurajima volcano, respectively. Similarly, MD982195 and the central part of Tanegashima Island lie c. 180 km northwest and c. 80 km east of the N-Ym source vent, Noike vent on Kuchierabujima Island, respectively. Tephtras Sz-S and N-Ym thus were distributed in various directions from the source volcanoes and their areas of distribution amount to more than 80,000 km<sup>2</sup> and 30,000 km<sup>2</sup>, respectively (Fig. 7). The VEIs for both are likely to be 6. In particular, tephra Sz-S extensively occurs not only over all of terrestrial southern Kyushu, but also in the northern part of the East China Sea and Pacific Ocean off southern Kyushu. Further investigations on cryptotephtras over more distant areas will enable the distribution of both tephtras to be mapped even further afield (e.g. Lowe, 2011).

#### 4.3. Palaeoenvironmental changes and cultural events

Tephra Sz-S has been widely recognised on land in southern Kyushu and utilised as a prominent time-parallel marker for precisely correlating and dating palaeoenvironmental and human records (Moriwaki et al., 2010).

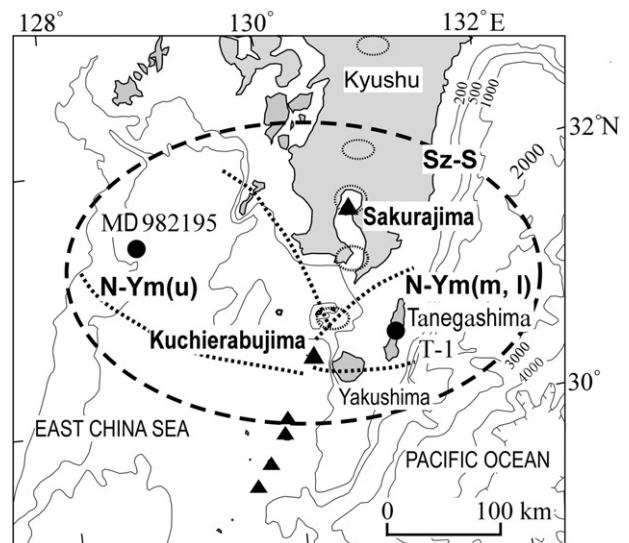


Fig. 7. Approximate distributions of Sakurajima-Satsuma (Sz-S) and Noike-Yumugi (N-Ym) tephtras. N-Ym (u) denotes the upper unit and N-Ym (m, l) denotes the middle/lower units of N-Ym. Broken and dotted lines show the approximate extents of tephtras Sz-S and N-Ym, respectively.

Kameyama et al. (2005) indicated that Aira caldera was submerged under seawater between about 11,700 and 11,000  $^{14}\text{C}$  BP. Such submergence was likely a consequence of the collapse of the southern caldera wall as a result of the Sz-S eruption. On the other hand, tephra Sz-S occurs in the coastal-lowland deposits of the last deglaciation in southern Kyushu, and the stratigraphic relation of tephra Sz-S to the depositional history and sea-level change shows that the relative sea-level at the time of Sz-S lies  $\sim 50$  m below present sea-level on the coastal lowland and that the evidence of initial marine invasion of the coastal lowland lies  $\sim 4$  m below Sz-S (Moriwaki et al., 2005). These findings show therefore that the marine invasion of Aira caldera within Kagoshima Bay occurred before the Sz-S eruption (Moriwaki et al., 2005), indicating that the inundation was not due to the collapse of caldera wall at the time of the Sz-S eruption. The stratigraphic position of tephra Sz-S, based on correlation of the marine oxygen isotope record of MD982195 to that of NGRIP (GICC05), demonstrates that the transgression likely reflects rapid sea-level rise caused by melt-water pulse 1a (Fairbanks, 1989; Bard et al., 1996). The occurrence of the 'wet' phreatomagmatic eruptions of Sz-S suggests that these eruptions involved seawater interaction with magma and thus took place when sea-level was  $\sim 50$  m below the present level (Moriwaki, 1994).

In terms of human culture, tephra Sz-S is a critical isochron for marking the stratigraphic position of the end of the microblade culture, the beginning of housing settlement, and the beginning of ceramic culture in southern Kyushu (Moriwaki et al., 2010), which were prominent changes for prehistoric archaeology of Japan.

## 5. Conclusions

Key marker tephtras of the last deglaciation, the Sakurajima-Satsuma (Sz-S) tephra from Sakurajima volcano and the Noike-Yumugi (N-Ym) tephra from Kuchierabujima Island, were identified in a marine core (IMAGES MD982195) in northern part of the East China Sea and on central Tanegashima Island on the basis of glass-chemical composition and stratigraphic associations. Sz-S tephra is rhyolitic and homogeneous in glass major-element composition. N-Ym is also rhyolitic, but diverse in composition both

stratigraphically as well as within individual clasts. Stratigraphically, tephra Sz-S, dated at 12,800 cal BP, occurs at around the start of the late-glacial reversal (cooling) in oxygen isotope records of MD982195 (Ijiri et al., 2005), which corresponds to the end of GI-1 and the start of GS-1 in the ice-core events of NGRIP (GICC05) (Lowe, J. et al., 2008). Tephra N-Ym, erupted before tephra Sz-S, marks the end of GI-1 as determined for MD982195 and thus has an age of ~13,000 cal BP based on the oxygen isotope stratigraphy in MD982195. However, an age of between 14,500 and 14,900 cal BP has been obtained for proximal N-Ym tephra, and so there is a discrepancy with these records. Either the identification of MD982195-B is incorrect or the ages are not correct, or both. Alternatively, part of core MD982195 may be missing (as can occur, e.g., see Carter et al., 1995). Tephra MD982195-C, close to ~20,000 cal BP on the basis of its position in MD982195 (Fig. 6), currently remains uncorrelated.

The occurrences of Sz-S and N-Ym tephras in core MD982195 and on Tanegashima Island reveal that those tephras are more widespread than previously demonstrated. The distal ash of Sz-S is likely sourced from the fall-out pumice units of proximal deposits. Glass chemical compositions of stratigraphically distinguishable units of N-Ym tephra suggest that the lower and middle units of N-Ym fall beds were dispersed to the east whereas the upper beds of N-Ym were dispersed to the north to northwest.

The distributions and stratigraphic positions in the oxygen isotope records of marine core MD982195 mean that these two newly identified tephras, Sz-S and N-Ym, together with AT and K-Ah, can help refine the chronology of the terrestrial palaeoenvironmental and archaeological records in southern Kyushu. These identifications form part of the programme to develop a more detailed chronostratigraphic framework for the Kyushu-INTIMATE project targeting the past 30,000 years.

## Acknowledgments

We are grateful to John Westgate (University of Toronto) for his suggestion to undertake glass-shard major element analyses of the tephras as reported here, and to Tadamichi Oba for his suggestion to obtain tephra samples. We thank Tetsuo Kobayashi for providing information on the ages of terrestrial tephras. We are also very grateful for helpful comments on the paper by anonymous referees. A fellowship from the Japan Society for the Promotion of Science permitted David J. Lowe to visit Japan in May, 2010, and that support is gratefully acknowledged. Part of the research was supported by a grant-in-aid for the Japan Society for the Promotion of Science, No. 21501001. This paper is an output associated with the INTREPID project (INQUA-0907), “Enhancing tephrochronology as a global research tool through improved fingerprinting and correlation techniques and uncertainty modeling”, which is supported by the International Union for Quaternary Research.

## References

- Alloway, B.V., Lowe, D.J., Barrell, D.J.A., Newnham, R.M., Almond, P.C., Augustinus, P.C., Bertler, N.A., Carter, L., Litchfield, N.J., McGlone, M.S., Shulmeister, J., Vandergoes, M.J., Williams, P.W., NZ-INTIMATE members, 2007. Towards a climate event stratigraphy for New Zealand over the past 30,000 years (NZ-INTIMATE project). *Journal of Quaternary Science* 22, 9–35.
- Arai, F., Oba, T., Kitazato, Y., Horibe, Y., Machida, H., 1981. Late Quaternary tephrochronology and palaeoceanography of the sediments of the Japan Sea. *The Quaternary Research of Japan* 20, 209–230 (in Japanese, with English Abstract).
- Bard, E., Hamelin, B., Arnold, M., Montaggioni, L., Cabioch, G., Faure, G., Rougerie, F., 1996. Deglacial sea-level record from Tahiti corals and the timing of global meltwater discharge. *Nature* 382, 241–244.
- Björck, S., Walker, M.J.C., Wynn, L.C., Johnsen, S., Knudsen, K.L., Lowe, J.J., Wohlfarth, B., INTIMATE members, 1998. An event stratigraphy for the last termination in the North Atlantic region based on the Greenland ice-core record: a proposal by the INTIMATE group. *Journal of Quaternary Science* 13, 283–292.
- Blockley, S.P.E., Bronk Ramsey, C., Lane, C.S., Lotter, A.F., 2008. Improved age modelling approaches as exemplified by the revised chronology for the central European varved lake Soppensee. *Quaternary Science Reviews* 27, 61–71.
- Carter, L., Nelson, C., Neil, H.L., Froggatt, P.C., 1995. Correlation, dispersal, and preservation of the Kawakawa Tephra and other late Quaternary tephra layers in the southwest Pacific Ocean. *New Zealand Journal of Geology and Geophysics* 38, 29–46.
- Fairbanks, R.G., 1989. Glacio-eustatic record 0–16,000 years before present: influence of glacial melting rates on Younger Dryas event and deep ocean circulation. *Nature* 34, 637–642.
- Geshi, N., Kobayashi, T., 2006. Volcanic activities of Kuchinoerabujima Volcano within the last 30,000 years. *Bulletin of the Volcanological Society of Japan* 51, 1–20 (in Japanese, with English Abstract).
- Hayashi, R., Takahara, H., Hayashida, A., Takemura, K., 2010. Millennial-scale vegetation changes during the last 40,000 yr based on a pollen record from Lake Biwa, Japan. *Quaternary Research* 74, 91–99.
- Hoek, W.Z., Yu, Z.C., Lowe, J.J., 2008. INTegration of ice-core, MARine and TERrestrial records (INTIMATE): refining the record for the last glacial-interglacial transition. *Quaternary Science Reviews* 27, 1–5.
- Ijiri, A., Wan, L., Oba, T., Kawahata, H., Huang, C.-Y., Huan, C.-Y., 2005. Paleoenvironmental changes in the northern area of the East China Sea during the past 42,000 years. *Palaeogeography, Palaeoclimatology, Palaeoecology* 219, 239–261.
- Kameyama, S., Shimoyama, S., Miyabe, S., Miyata, Y., Sugiyama, T., Iwano, H., Danhara, T., Endo, K., Matsukuma, A., 2005. Stratigraphy and ages of Aira caldera deposits in Shinjima (Moesjima), Kagoshima prefecture, west Japan. *The Quaternary Research of Japan* 44, 15–19 (in Japanese, with English Abstract).
- Kawahata, H., Oshima, H., 2004. Vegetation and environmental record in the northern East China Sea during the late Pleistocene. *Global and Planetary Change* 41, 251–273.
- Kawahata, H., Nohara, M., Aoki, K., Minoshima, K., Gupta, L., 2006. Biogenic and abiogenic sedimentation in the northern East China Sea in response to sea-level change during the late Pleistocene. *Global and Planetary Change* 53, 108–121.
- Kitagawa, H., Fukusawa, H., Nakamura, T., Okamura, M., Takemura, K., Hayashida, A., Yasuda, Y., 1995. AMS <sup>14</sup>C dating of varved sediments from Lake Suigetsu, central Japan and atmospheric <sup>14</sup>C change during the late Pleistocene. *Radiocarbon* 37, 371–378.
- Kobayashi, T., 1986. Volcanic history and pyroclastic flows of Sakurajima Volcano. In: Aramaki, S. (Ed.), *Characteristics of Dry High Concentration Flows (Pyroclastic Flows) Associated with Volcanic Eruption and Their Disasters*, pp. 137–163 (in Japanese).
- Kobayashi, T., Okuno, M., Nakamura, T., 2002. Eruption history of Kuchierabu volcano. In: Satsuma-Iojima kasan, Kuchierabujima kasan no shuchu sogo kansoku. Sakurajima Volcano Research Center, Disaster Prevention Research Institute Kyoto University, pp. 169–178 (in Japanese).
- Kobayashi, T., Tameike, T., 2002. History of eruptions and volcanic damage from Sakurajima Volcano, southern Kyushu, Japan. *The Quaternary Research of Japan* 41, 269–278 (in Japanese, with English Abstract).
- LeBas, M.J., LeMaitre, R.W., Streckeisen, A., Zanettin, B., 1986. A chemical classification of volcanic rocks based on the total alkali-silica diagram. *Journal of Petrology* 27, 745–750.
- Lowe, D.J., 2011. Tephrochronology and its application: a review. *Quaternary Geochronology* 6, 107–153.
- Lowe, D.J., Shane, P.A.R., Alloway, B.V., Newnham, R.M., 2008. Fingerprints and age models for widespread New Zealand tephra marker beds erupted since 30,000 years ago: a framework for NZ-INTIMATE. *Quaternary Science Reviews* 27, 95–126.
- Lowe, J.J., Hoek, W.Z., INTIMATE group, 2001. Inter-regional correlation of palaeoclimatic records for the Last Glacial-Interglacial Transition: a protocol for improved precision recommended by the INTIMATE project group. *Quaternary Science Reviews* 20, 1175–1187.
- Lowe, J.J., Rasmussen, S.O., Björck, S., Hoek, W.Z., Steffensen, J.P., Walker, M.J.C., Yu, Z.C., INTIMATE group, 2008. Synchronisation of palaeoenvironmental events in the North Atlantic region during the Last Termination: a revised protocol recommended by the INTIMATE group. *Quaternary Science Reviews* 27, 6–17.
- Machida, H., 2010. Outline of tectonic setting and explosive volcanism of southern Kyushu. In: Moriwaki, H., Lowe, D.J. (Eds.), *Intra-conference Field Trip Guides. INTAV International Field Conference on Tephrochronology, Volcanism, and Human Activity*, Kirishima City, Kyushu, Japan, 9–17 May, 2010, pp. 11–35.
- Machida, H., Arai, F., 1983. Extensive ash falls in and around the Sea of Japan from large late Quaternary eruptions. *Journal of Volcanology and Geothermal Research* 18, 151–164.
- Machida, H., Arai, F., 1992. Atlas of Tephra in and around Japan. University of Tokyo Press, Tokyo (in Japanese).
- Machida, H., Arai, F., 2003. Atlas of Tephra in and around Japan [revised edition]. University of Tokyo Press, Tokyo (in Japanese).
- Machida, H., Arai, F., Lee, B.-S., Moriwaki, H., Furuta, T., 1984a. Late Quaternary tephras in Ulreung-do island, Korea. *Journal of Geography of Japan* 93, 1–14 (in Japanese, with English Abstract).
- Machida, H., Arai, F., Sugihara, S., Oda, S., Endo, K., 1984b. Tephra and Japan archaeology - Tephra Catalogue related to archaeological research. In: Watanabe, N. (Ed.), *General Report on Conservation Science Related to Cultural Properties and Human and Natural Science*, pp. 865–928. Tefura to Nihon Kokogaku - Kokogaku Kenkyu to kankeisuru Tefura no Katarogu -. Watanabe N.

- (ed.) Kobunkazai ni kansuru Hozonkagaku to Jinbun-Shizen Kagaku - Sokatsu Hokokusho -, 865-928 (in Japanese).
- Moriwaki, H., 1992. Late Quaternary phreatomagmatic tephra layers and their relation to paleo-sea levels in the area of Aira caldera, southern Kyushu, Japan. *Quaternary International* 13/14, 195–200.
- Moriwaki, H., 1994. Palaeoenvironmental Study on Late Quaternary Fine Ash Beds around Kagoshima Bay. Reports for Grants-in-Aid for Scientific Research (no. 04680248) from Ministry of Education (in Japanese).
- Moriwaki, H., 2010. Late Pleistocene and Holocene tephra in southern Kyushu. In: Moriwaki, H., Lowe, D.J. (Eds.), Intra-conference Field Trip Guides. INTAV International Field Conference on Tephrochronology, Volcanism, and Human Activity, Kirishima City, Kyushu, Japan, 9–17 May, 2010, pp. 44–53.
- Moriwaki, H., Nagasako, T., Arai, F., 2009. Late Pleistocene and Holocene tephra in the Tokara islands, southern Japan. *The Quaternary Research of Japan* 48, 271–287 (in Japanese, with English Abstract).
- Moriwaki, H., Nakamura, N., Sangawa, T., 2010. Tephra and archaeology in southern Kyushu. In: Moriwaki, H., Lowe, D.J. (Eds.), Intra-conference Field Trip Guides. INTAV International Field Conference on Tephrochronology, Volcanism, and Human Activity, Kirishima City, Kyushu, Japan, 9–17 May, 2010, pp. 71–75.
- Moriwaki, H., Ohira, A., Matsushima, Y., Oki, K., 2005. Tephrochronology of Holocene deposits and palaeoenvironmental change in Kokubu lowland, southern Kyushu, Japan. Abstract for the Congress of Japan Association for Quaternary Research, No. 35, 131–132 (in Japanese).
- Nakagawa, T., Kitagawa, H., Yasuda, Y., Tarasov, P.E., Gotanda, K., Sawai, Y., 2005. Pollen/event stratigraphy of the varved sediment of Lake Suigetsu, central Japan from 15,701 to 10,217 SG kyr BP (Suigetsu varve years before present): description, interpretation, and correlation with other regions. *Quaternary Science Reviews* 24, 1691–1701.
- Newnham, R.M., Eden, D.N., Lowe, D.J., Hendy, C.H., 2003. Rerewhakaaitu Tephra, a land-sea marker for the Last Termination in New Zealand, with implications for global climate change. *Quaternary Science Reviews* 22, 289–308.
- Okuno, M., 2002. Chronology of tephra layers in southern Kyushu, SW Japan, for the last 30,000 years. *The Quaternary Research of Japan* 41, 225–236 (in Japanese, with English Abstract).
- Okuno, M., Nakamura, T., Moriwaki, H., Kobayashi, T., 1997. AMS radiocarbon dating of the Sakurajima tephra group, southern Kyushu, Japan. *Nuclear Instruments and Methods in Physics Research B* 123, 470–474.
- Okuno, M., Shiihara, M., Torii, M., Nakamura, T., Kim, K., Domitsu, H., Moriwaki, H., Oda, M., 2010. AMS radiocarbon dating of the Holocene tephra layers on Ulleung island, south Korea. *Radiocarbon* 52, 1465–1470.
- Rasmussen, S.O., Andersen, K.K., Svensson, A.M., Steffensen, J.P., Vinther, B., Clausen, H.B., Siggaard-Andersen, M.-L., Johnsen, S.J., Larsen, L.B., Dahl-Jensen, D., Bigler, M., Röthlisberger, R., Fischer, H., Goto-Azuma, K., Hansson, M., Ruth, U., 2006. A new Greenland ice core chronology for the last glacial termination. *Journal of Geophysical Research* 111, D06102.
- Rasmussen, S.O., Seierstad, I.K., Anderson, K.K., Bigler, M., Dahl-Jensen, D., Johnsen, S.J., 2008. Synchronization of the NGRIP, GRIP, and GISP2 ice cores across MIS 2 and palaeoclimatic implications. *Quaternary Science Reviews* 27, 18–28.
- Shane, P.A.R., Smith, V.C., Lowe, D.J., Nairn, I.A., 2003. Re-identification of c. 15 700 cal BP tephra bed at Kaipo Bog, eastern North Island: implications for dispersal of Rotorua and Puketarata tephra beds. *New Zealand Journal of Geology and Geophysics* 46, 591–596.
- Shane, P.A.R., Nairn, I.A., Martin, S.B., Smith, V.C., 2008. Compositional heterogeneity in tephra deposits resulting from the eruption of multiple magma bodies: implications for tephrochronology. *Quaternary International* 178, 44–53.
- Turney, C.S.M., van den Burg, K., Wastegård, S., Davies, S.M., Whitehouse, N.J., Pilcher, J.R., Callaghan, C., 2006. North European last glacial–interglacial transition (LGIT; 15–9 ka) tephrochronology: extended limits and new events. *Journal of Quaternary Science* 21, 335–345.
- Wohlfarth, B., Blaauw, M., Davies, S.M., Andersson, M., Wastegård, S., Hormes, A., Posnert, G., 2006. Constraining the age of Lateglacial and early Holocene pollen zones and tephra horizons in southern Sweden with Bayesian probability methods. *Journal of Quaternary Science* 21, 321–334.